

# Optical Injection-Locked Directly Modulated Lasers for Dispersion Pre-Compensated Direct-Detection Transmission

Zhixin Liu , Senior Member, IEEE, Senior Member, OSA, Graham Hesketh, Brian Kelly , Member, IEEE, John O'Carroll, Member, IEEE, Richard Phelan , David J. Richardson , Fellow, IEEE, Fellow, OSA, and Radan Slavík , Senior Member, IEEE, Fellow, OSA

**Abstract**—The growing traffic demand in interdata center and metro communications requires high-speed and low-cost transceivers that can flexibly adapt to different transmission distances of up to a few hundred km. Ultimately low-cost transceivers will use the simplest optical hardware, namely a directly modulated transmitter and direct detection receiver. Using optical injection-locked directly modulated lasers, we propose a transmitter that can control the full field of the optical signal and achieve error-free transmission over up to 300 km of dispersion uncompensated SMF-28. We demonstrate such a transmission system and discuss its potential for short- and medium-reach communication systems.

**Index Terms**—Data center interconnection, digital signal processing (DSP), directly modulated laser (DML), metro networks, optical injection locking, optical transmitters, pulse amplitude modulation (PAM).

## I. INTRODUCTION

THE unprecedented growth of data that needs to be stored and transmitted in data centers (DCs) and metro networks is driving the quest for fast and inexpensive optics to facilitate high-speed communications over distances ranging from 70 km to up to 300 km [1]. Although the requirements on data rate and transmission distance can be readily achieved using sophisticated coherent communication technologies, the cost and power consumption of the coherent optical transceivers are inherently higher than their direct-modulation direct-detection (DM-DD) counterparts. Undoubtedly, metro-distance optical communications systems will be more cost and energy efficient if DM-DD

transceivers can be developed to meet the data rate and transmission distance requirements.

For this reason, there is a surge in research on transmitter and modulation techniques for high-speed DD transmission systems, with a focus on mitigating or compensating for the impairments caused by chromatic dispersion (CD) [2]–[4] which normally severely limits the capacity-reach product of DD systems. Using the single-sideband (SSB) discrete multitone (DMT) modulation format in conjunction with Kramers-Kronig digital signal processing (DSP), researchers have demonstrated a single-wavelength net rate of 256 Gb/s over 125 km of standard single mode fiber (SMF-28) [2], [3]. In [4], a  $4 \times 112$  Gb/s data rate over 240 km SMF-28 was demonstrated using SSB subcarrier modulation (SCM) with Kramers-Kronig DSP. Although the above-mentioned technologies only require a simple photodetector, their transmitters use a standard LiNbO<sub>3</sub> In-phase (I) and Quadrature (Q) modulator that is bulky, expensive, and requires relatively high RF power at its input. Additionally, the receiver-side Kramers-Kronig detection used requires a high oversampling ratio analog-to-digital converter (ADC) and a heavy DSP load that increases power consumption and cost. This goes against the goal of employing direct detection for low-cost and low power consumption transceivers.

The ultimate simplification (and thus cost, size, and power consumption reduction) would be realized if DM-DD transceiver could be used with a simple modulation format such as 4-level pulse amplitude modulation (PAM4). Compared to DMT and SCM formats, PAM4 can be demodulated using pure analog electronics without DSP, which greatly reduces the transceiver cost and power consumption. Such a solution has been adopted for short-reach intra-DC interconnection [5]. Currently, researchers are actively developing PAM4 transmission for >100 km transmission distance [6], [7].

As regards to DMLs themselves, recent advances have demonstrated up to 55 GHz modulation bandwidth for 2-km short reach communications [8]. The transmission distance here, is limited by the fiber CD and its interplay with the frequency chirp associated with the direct laser modulation. Indeed, CD is the main challenge for DMLs in metro-distance transmission systems that operate at the low-loss 1550 nm wavelength region. To compensate for the CD, dispersion compensating fiber (DCF) was employed in a 100-km  $8 \times 25$  Gb/s

Manuscript received March 22, 2018; revised July 5, 2018; accepted August 19, 2018. Date of publication August 23, 2018; date of current version September 12, 2018. This work was supported in part by the EPSRC Fellowship Grant agreement EP/K003038/1, Photonic Hyperhighway EP/I061196X, EPSRC New Investigator Award EP/R041792/1, and in part by the Royal Society Research Grant RSG\R1\180200. (Corresponding author: Zhixin Liu.)

Z. Liu is with the Department of Electronic and Electrical Engineering, University College London, London WC1E 7JE, U.K. (e-mail: zhixin.liu@ucl.ac.uk).

G. Hesketh, D. J. Richardson, and R. Slavik are with the Optoelectronics Research Centre, University of Southampton, Southampton SO17 1BJ, U.K. (e-mail: gdh1e10@gmail.com; djr@orc.soton.ac.uk; R.Slavik@soton.ac.uk).

B. Kelly, J. O'Carroll, and R. Phelan are with the Eblan Photonics, Dublin A96 A621, Ireland (e-mail: brian.kelly@eblanaphotonics.com; john.ocarroll@eblanaphotonics.com; richard.phelan@eblanaphotonics.com).

Color versions of one or more of the figures in this paper are available online at <http://ieeexplore.ieee.org>.

Digital Object Identifier 10.1109/JLT.2018.2866832

PAM4 transmission experiment [6]. However, the use of DCF increases the system cost, reduces the optical signal-to-noise ratio (OSNR) after transmission, and most importantly, it limits network flexibility (e.g., making signal re-routing through a different path challenging). To minimize the adverse effect of fiber CD, optical filtering has been explored to reshape the optical spectrum to generate vestigial sideband (VSB) or duobinary signals [9], [10]. A data rate of up to 56 Gb/s has been achieved for transmission over 100-km of SMF-28 by aligning the laser wavelength to the filter edge of a delay interferometer [9]. The chirp managed laser co-packages an optical filter in the laser module and a maximum distance of 200-km has been achieved using 10-Gb/s duobinary format signaling [10]. Nevertheless, these techniques can only reduce the signal's sensitivity to CD. It would be more desirable if one could achieve full compensation of CD rather than minimizing its effect.

In this paper, we report on a DML-based transmitter scheme that allows for full-field optical modulation and full compensation of CD for intensity-modulated signals. The proposed transmitter employs two optically injection-locked directly-modulated lasers (OIL-DML) to generate amplitude-modulated signals with a controllable phase profile, i.e., modulation of the I and Q components using independent lasers. With the capability of full field modulation, the transmitter compensates for CD using transmitter-side DSP and enables error-free direct-detection of 20-Gb/s PAM4 signals after transmission over up to 300-km of SMF-28. The moderate data rate was due to the bandwidth limitation of the low-cost Fabry-Perot laser diodes used in the experiment. Researchers have experimentally demonstrated up to 80 GHz modulation bandwidth using injection-locked lasers, showing great potential for applying the proposed transmitter scheme to high-speed transmission systems [11].

The concept of the proposed transmitter was first reported at OFC 2017 [12]. This paper extends the conference abstract by explaining the impact of residual chirp on an OIL-DML, the method that we propose to characterize the amplitude-phase response, and the digital signal processing approach that compensates for the complex amplitude-phase distortion. The additional material included in this paper, in conjunction with the more detailed description of our experimental setup and results, give greater insight into the considerations and challenges of OIL-DML based transceivers.

This rest of this paper is organized as follows. Section II explains the operational principle of the proposed transmitter. Section III describes the transmitter-side DSP with a focus on the method we developed to compensate for the residual chirp induced nonlinear amplitude-phase response of the OIL-DMLs. Sections IV and V describes the proof-of-concept experiment and results, respectively. Finally, we conclude this paper in Section VI.

## II. OPERATIONAL PRINCIPLE OF THE PROPOSED TRANSMITTER

### A. Transmitter Schematic

Fig. 1(a) shows a schematic diagram of the proposed transmitter. The principle of operation is explained using constellation diagrams for PAM4 signal generation, in which the orange

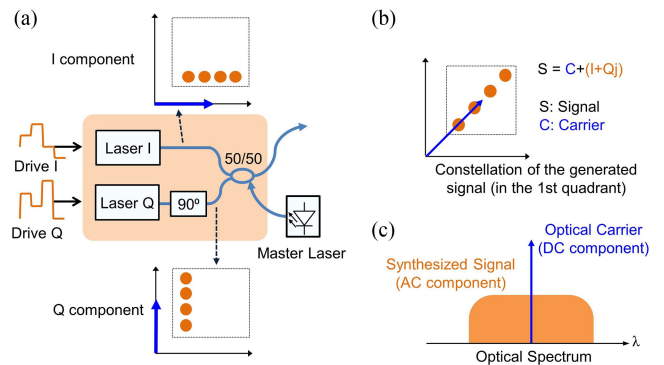


Fig. 1. Operational principle of the proposed transmitter. (a) Schematic diagram; (b) constellation of the generated signal using PAM4 as the example; (c) the spectrum of the generated signal (lower figure). The optical carrier is represented by the blue arrow and the signal component (AC component) is represented in orange.

points represent the constellation of the optical signals. Our transmitter consists of two slave DMLs (Laser I and Laser Q) that are injection-locked by the same master laser. Under OIL, the chirp is suppressed and the DMLs become mutually coherent. Therefore, the outputs of the DMLs can be combined orthogonally by introducing a  $90^\circ$  phase shift to the Q arm, yielding a complex (amplitude and phase) modulated signal, as indicated by the orange part of the constellation in Fig. 1(b). Since direct laser modulation is essentially intensity modulation, the constellation of the synthesized signal lies in the first quadrant of the complex plane and its optical spectrum contains a carrier component (the blue arrows in Fig. 1). This transmitter configuration provides the capability to manipulate both In-phase and Quadrature (I-Q) components of the synthesized signal, thereby enabling the CD to be pre-compensated at the transmitter side for an intensity-modulated signal. In principle, this scheme allows for pre-compensation of any deterministic impairment, such as chromatic dispersion, fiber nonlinearity interference (e.g., self-phase modulation), and electronic signal distortions including harmonic distortion in the RF amplifiers and quantization interference in the digital-to-analog converters (DACs). Thus, we can transmit DD PAM signals over long distance without using DCF. Besides, this transmitter also harvests the various benefits of optical injection locking, including an enhanced modulation bandwidth [13], a reduced relative intensity noise and laser linewidth [14]. Compared to our previously published coherent transmitter in [15], the scheme here simplifies the transmitter by removing the need to reflect the continuous wave (CW) portion of the master laser radiation to provide carrier suppression through destructive interference, offering a full-field modulation with an optical carrier for DD of intensity modulated signals.

### B. Residual Chirp of Injection-Locked DML

Although the suppression of the modulation chirp using OIL has enabled coherent synthesis of quadrature phase shift keying (QPSK) and 16 quadrature amplitude modulation (16-QAM) signals, the generated signal still experiences residual chirp that causes additional phase modulation [15], [16]. In Fig. 2 we

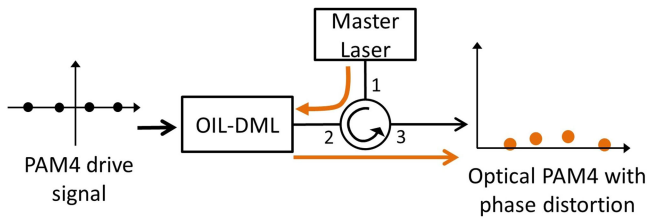


Fig. 2. Non-linear field response of an OIL-DML using PAM4 as the example. Black points: constellation of the electrical driving signals; Orange points: constellation of the generated optical signals.

explain the signal distortion caused by the residual chirp using a PAM4 constellation diagram. The black points on the left represent the constellation of the 4-level electrical signal that drives the OIL-DML. The output optical PAM4 signal has four intensity levels with phase distortion as depicted using the orange points on the right. After direct modulation, phase distortion is imparted on the optical signal leading to a distorted constellation.

In a coherent transmission system, this field distortion can be post-compensated using receiver-side digital equalizers [15]. In a DD system, however, this nonlinear field distortion is detrimental because the CD-precompensated signals require a linear mapping from the digital domain to the optical domain. Therefore, the generation of CD pre-compensated signals requires correction of this nonlinear field response to generate a rectilinear constellation diagram in the optical domain.

### III. DIGITAL SIGNAL PROCESSING FOR IMPAIRMENT COMPENSATION

The residual chirp of an OIL-DML under strong light injection was first explored by Yabre using numerical methods [16]. Lau *et al.* conducted an analytical study that uses chirp-to-power ratio (CPR) as a figure-of-merit and associates the CPR to a number of laser parameters, including the injection ratio, laser linewidth enhancement factor, photon and carrier lifetime, gain coefficient, threshold density, gain compression factor, and the phase and frequency deviation between the master and slave light [14].

Although this analytical result reveals the physical origin of the residual chirp, it is very challenging to implement the analytical model for the digital pre-distortion, because the required laser parameters are extremely difficult to measure with sufficient precision. In practice, accurate characterization of all the parameters of each laser chip would significantly increase the cost, which is against our goal of producing a simple and cost-effective transceiver.

To efficiently compensate for the residual chirp, we propose here to consider the amplitude-phase response of an OIL-DML as a black box, and to employ a numerical approach instead of the analytical model. Using this approach, the nonlinear distortion can be effectively compensated without measuring specific laser parameters. The proposed method contains three steps: 1) measuring the full-field nonlinear response of the proposed transmitter; 2) based on the measured data set, calculating a 2-D mapping data set that compensates for the nonlinear field

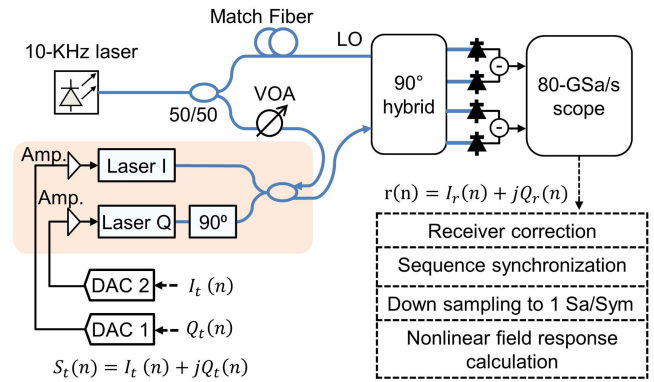


Fig. 3. Experimental setup for transmitter amplitude-phase response characterization. VOA: variable optical attenuator; DAC: digital-to-analog converter; LO: local oscillator; Amp.: RF amplifier.

response; 3) generating pre-distorted electrical drive signals that compensate for the CD and the nonlinear field modulation.

#### A. Measurement of the Amplitude-Phase Response

We employed homodyne coherent detection to measure the nonlinear field response of the proposed transmitter. The experimental setup is shown in Fig. 3. A 10-kHz narrow linewidth laser emitting 13 dBm of laser power at 1556 nm was split into two branches: one was used as the local oscillator (LO) and the other as the master beam for the OIL. In the experiment, we used a narrow linewidth laser to facilitate the homodyne coherent detection that characterizes the amplitude-phase response. In a practical transmitter, a relatively large linewidth laser can be used with sufficiently good performance [17], allowing for a potential fully integrated transmitter. A variable optical attenuator (VOA) was used to set the injection power to 3 dBm. The two slave DMLs were low-cost FP-LD packaged without isolators to enable OIL. Both DMLs were biased at 45 mA, which is four times higher than their threshold currents. Without OIL, their modulation bandwidths were very small - merely 1.8 GHz. To simultaneously enhance their modulation bandwidth and reduce the chirp, the injected master light carrier frequency was tuned about 10 GHz higher than the natural frequency of the slave lasers [14]. After OIL, the FP-LDs lase at the master frequency with an output power of 7 dBm. The OIL-DMLs were modulated by training signals generated by two independent digital-to-analog converters (DACs) operating at a fixed sampling rate of 92 GS/s and a peak-to-peak voltage ( $V_{pp}$ ) of 1.8 V. The output signals from both lasers have an extinction ratio (ER) of about 2.5 dB. We employed 81-QAM as a training signal, whose constellation diagram is shown in Fig. 4(a). 28000 training symbols were used to calculate the nonlinear field response of the proposed transmitter. In the upper branch, a short fiber was used to minimize the difference in optical path length between the upper and lower branches such that the signal and LO have sufficient coherence for homodyne coherent detection. The optical fiber and components in the setup are all polarization maintaining (PM) for the use of a single-polarization coherent receiver for signal detection. The DC component of the detected signal was canceled using a balanced detector and the AC component was

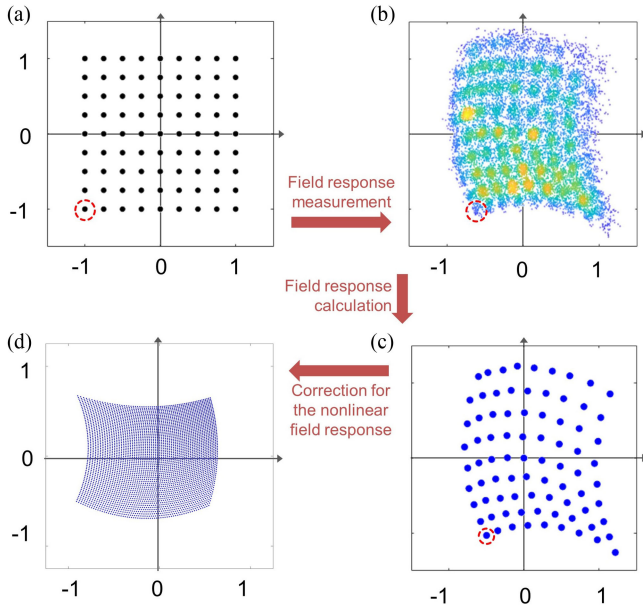


Fig. 4. Explanation of calculating the nonlinear pre-compensation coefficient using constellation diagrams: (a) Constellation diagram of the training symbols (81QAM); (b) The detected training signal using the homodyne coherent receiver; (c) The calculated amplitude-phase response; (d) the calculated pre-distortion coefficients assuming using 8-bit DACs.

subsequently digitized using an 80-GSa/s real-time oscilloscope before the off-line DSP. It is worth noting that although in principle intradyne detection could be used, it lacks practicality in the experiment due to the limited number of bits of the analog-to-digital converters (ADCs) in the real-time oscilloscope. The carrier-LO beating in an intradyne receiver will generate strong sinusoid terms that result in a limited SNR for the signal (AC) components. The homodyne detection, however, cancels this carrier-LO beating (the DC term of the detected signal) in the balanced detectors and generates a high SNR AC component for the characterization of the amplitude-phase response of the OIL-DMLs.

The off-line DSP is shown in the dashed blocks in Fig. 3. It downsamples the detected signal to one sample per symbol and synchronizes it with the training symbols. We explain the DSP process using the normalized constellation diagrams of the synchronized signals in Fig. 4. Fig. 4(a) shows the constellation diagram of the 81QAM training signals. We choose 81QAM (9 levels for I and Q respectively) because it provides an appropriate trade-off between the computation complexity and accuracy of the field response characterization. Other constellations such as 64QAM, which provides 8-level digital quantization in the I and Q components, can also be used, which gives lower complexity in the nonlinear pre-distortion process detailed below, but at the expense of slightly lower accuracy.

Fig. 4(b) shows the constellation diagram of the detected training signals using the homodyne coherent receiver. The calculated nonlinear field response and the pre-compensation coefficient are shown in Fig. 4(c) and Fig. 4(d), respectively. Here we use the constellation point  $-1 -1j$  as an example to explain how we calculate the nonlinear field response. In the experiment, the  $-1 -1j$  symbol corresponds to a drive voltage of  $-0.9$  V for

both OIL-DMLs. After modulation, the detected symbols corresponding to the  $-1 -1j$  symbol are shown as the lower left cluster in Fig. 4(b) (highlighted with red circle) and were subsequently averaged to get the nonlinear field response, as highlighted with the red circle in Fig. 4(c). The field responses for the other constellation points were obtained in the same way. Mathematically, the obtained 2-D constellation mapping  $R(I, Q)$  as shown in Fig. 4(c) is the response of the square constellation points  $S(I, Q)$  in Fig. 4(a), in which  $I$  and  $Q$  are the coordinates of the constellation points. It can be seen that both the amplitude and phase response of the complex field response  $R$  are nonlinear. The amplitude response is nonlinear because the laser current modulation changes the optical power (amplitude squared). The phase distortion is caused by the residual chirp. We also observe in Fig. 4(b) that the constellation clusters are more converged in the lower left side (the 3rd quadrant) and become more diverged with an increase in the drive voltage. This likely originates from both the laser power modulation and the dynamic laser response, which is governed by the OIL laser rate equation [18].

## B. Digital Pre-Compensation

Based on the data set of the measured nonlinear field response, we generate the corrected digital samples that compensate for the nonlinear field response. The correction method is described as follows:

Assuming  $(x, y)$  are the coordinates of the optical field in Fig. 4(a) and (d), and  $(X, Y)$  are the coordinates in Fig. 4(b) and (c). The coordinate  $(x, y)$  is mapped to  $(X, Y)$  by the nonlinear field response  $R$  (as shown in Fig. 4(c)), which we approximate with a 2-D polynomial  $P$ , that is:  $(X, Y) = R(x, y) \sim P(x, y)$ . Therefore, to achieve a desired output  $(X, Y)$  we can find the appropriate input  $(x, y)$  (shown in Fig. 4(d)) by inverting the map, obtaining:  $(x, y) = P^{-1}(X, Y)$ .

Using this method, the CD pre-compensated digital samples are corrected with the nonlinear field response, and subsequently generated by the DACs that were used to drive the OIL-DMLs. The DACs used in our experiment have 8 bits resolution. Therefore, we create a  $2^8 \times 2^8$  data set for the response correction coefficients as shown in Fig. 4(d). The resulting response correction coefficients can be efficiently implemented to correct for the nonlinear field response using a look-up table approach.

Indeed, direct laser modulation is inherently pattern dependent and is best described by the laser rate equation [16]. Simplifying the field response as an instantaneous nonlinear mapping process does not fully capture the pattern dependent effect. For example, the pattern dependent thermal chirp [19] that governs the low frequency amplitude-phase response may not be compensated using the proposed method in this paper. Limited by the memory size of the FPGA that drives the DACs, we were unable to experimentally investigate pattern-dependent effects. Nevertheless, the DSP technique proposed here proved to be an effective method as to be discussed in Section IV. Comparing to the analytical method, it offers a simple and efficient way to realize a reasonably linear mapping from the digital domain to the optical domain, allowing CD pre-compensation using the proposed transmitter. However, better performance

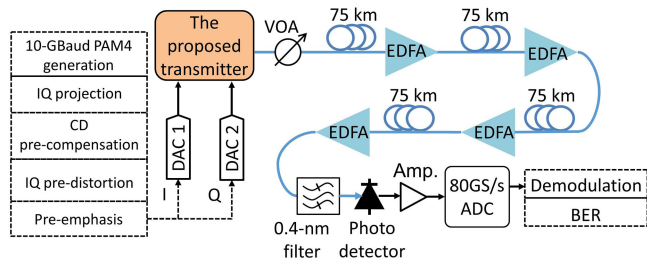


Fig. 5. Experimental setup for the proof-of-concept transmission experiment. CD: chromatic dispersion; EDFA: erbium-doped fiber amplifier; ADC: analog-to-digital converter; BER: bit error ratio.

can be expected if a multi-tap equalizer is employed, such as a Volterra filter, for the field pre-distortion. Commonly used coding technologies such as 8B10B coding can be employed to minimize the pattern-dependent effect.

It is also worth pointing out that the two slave lasers may have different modulation characteristics even if they are manufactured in the same batch. The DSP pre-distortion method also compensates for this difference in modulation response.

#### IV. SYSTEM EXPERIMENTAL SETUP

The experimental setup of our proof-of-concept transmission experiment is shown in Fig. 5. The transmitter described in Section III-A was driven by two 92-GSa/s DACs for In-phase and Quadrature components. The  $90^\circ$  phase shift between the two OIL-DML laser outputs was controlled via a piezoelectric (PZT)-driven fiber stretcher placed at the output of the Q arm. 1% of the combined optical signal was detected and used as an error signal that was fed back via a proportional-integral (PI) controller to keep the two slave lasers in quadrature. In this experiment, the relative phase was within  $90 \pm 3^\circ$ , ensuring sufficient orthogonality between the two OIL-DML outputs for I-Q modulation. The future fully integrated devices will enable simpler feedback control (due to short path lengths involved) and allow for a more accurate  $90^\circ$  phase shift between the I-Q components. In practice, a lower rate DAC would be sufficient (e.g., 25 GS/s, corresponding to a 2.5-time oversampling rate) for 20-Gb/s PAM4 transmission with negligible performance degradation [20].

The transmitter output power was 7 dBm. A VOA was used to change the power launched into the fiber link to control the OSNR after transmission. The transmission link comprised four spans of 75-km SMF-28 with an average CD coefficient of 16.8 ps/(nm·km). The link loss was compensated by in-line erbium-doped fiber amplifiers (EDFAs) with a noise figure of about 5 dB. After transmission, the signal was filtered by a 0.4-nm optical bandpass filter before direct detection. The detected electrical signal was captured by a 16-GHz, 80-GSa/s analog-to-digital converter (ADC). Signal demodulation, receiver-side equalization, and BER calculation were implemented using off-line DSP.

The driving waveforms for CD pre-compensated PAM4 signals were generated offline using a random bit sequence of  $2^{13} - 1$  length. The pattern length was limited by the

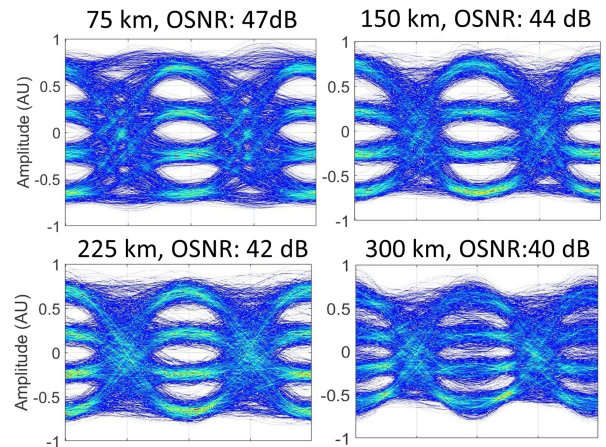


Fig. 6. Eye diagrams of the direct detected PAM4 signal and the OSNRs after transmission over different length of SMF-28.

DAC memory. The generated digital PAM4 symbols were oversampled to the DAC rate and projected onto the complex plane to generate the corresponding I and Q components of the synthesized signal, as shown in the conceptual diagram in Fig. 1. A digital finite impulse response (FIR) filter was implemented to compensate for the CD [21]. Afterwards, non-linear field distortion of the transmitter response was compensated using the amplitude-phase pre-distortion method described in Section III-B. Finally, a digital pre-emphasis filter was applied to compensate for the frequency roll-off of the signal path [22]. In principle, a nonlinear equalizer such as the Volterra filter could be used to realize the function of all the DSP pre-compensation blocks above.

At the receiver side, both fixed-threshold symbol detection and digital equalization were used to measure the bit error ratio (BER). The digital equalizer contained a 2-sample-per-symbol feed forward equalizer (FFE) and a 1-sample-per-symbol decision feedback equalizer (DFE) with 13 forward taps and 1 feedback tap. The BER was calculated by averaging 60 frames of different random bit sequences, which corresponds to 491460 bits.

#### V. RESULTS AND DISCUSSION

##### A. Experimental Results

Fig. 6 shows the eye diagrams of the direct-detected PAM4 signals after transmission over 75, 150, 225, and 300 km of SMF-28, respectively. The corresponding OSNR values were 47, 44, 42, and 40 dB, respectively. The degradation of the eye diagrams after long transmission distances are mainly due to the reduced OSNR, residual chirp and dispersion. The RF spectrum of the detected PAM4 signal after 300-km transmission is shown as the solid line in Fig. 7. For comparison, we plot the simulated RF spectrum of a chirp-free 20-Gb/s PAM4 signal generated by a push-pull MZM using a dashed line. Without CD compensation, multiple dips are observed for the MZM generated PAM4 signal due to CD-induced frequency fading. No such fading was observed in our experiment due to the pre-compensation of the CD. Under injection locking, the use of optical injection locking enhanced the lasers' modulation bandwidth from 1.8 GHz

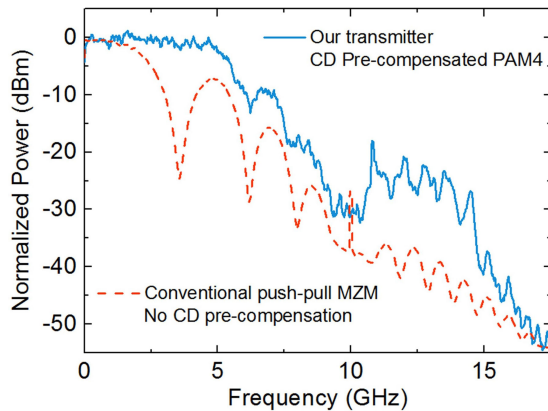


Fig. 7. RF spectrum of the detected signal after 300-km transmission. Solid line: Our transmitter with CD pre-compensation; Dashed line: Simulated push-pull MZM transmitter without CD compensation.

to about 7 GHz [14]. The frequency roll-off beyond 7 GHz was due to both laser packaging and the FP-LD design, which was not optimized for high-speed modulation.

Fig. 8(a) shows the BER obtained at different OSNR values using fixed-threshold detection. Error-free transmission (no error bit measured for half a million bits) was achieved for transmission up to 225 km and a BER of  $1.3 \times 10^{-3}$  was obtained after 300-km transmission, which is below the hard-decision FEC threshold of  $3.8 \times 10^{-3}$ . The required OSNRs for the BER of  $3.8 \times 10^{-3}$  were 36, 38.5, 40, and 40.5 dB, for the transmission distances of 75, 150, 225, and 300 km, respectively. The BER results with the FFE-DFE equalizer are plotted in Fig. 8(b). Using the simple equalizer, error-free transmission was achieved for all distances. The inset shows the equalized eye diagram after 300-km transmission. The required OSNRs for the BER of  $3.8 \times 10^{-3}$  were 35.5, 37.3, 37.5, and 38 dB, for the distances of 75, 150, 225, and 300 km, respectively. The OSNR penalty is likely due to the different modulation depth, residual chirp and CD, as the proposed DSP pre-distortion does not fully capture the laser dynamics.

### B. Discussion

The relatively high OSNR requirements in our experiment primarily result from the relatively small extinction ratio (ER, about 2.5 dB) that limited the SNR of the detected signal after transmission. This limitation was due to the availability of components, i.e., the FP-LDs were not designed for high-speed modulation and the RF voltage amplifiers have only 11 dB gain. Driving the lasers with higher RF power than that used in our experiment would increase the ER, which could in principle reduce the required OSNR after transmission. However, increasing the ER also introduces stronger modulation chirp that distorts the constellation diagram [23]. This trade-off between the ER and modulation chirp can in our view be unlocked by: 1) adding carrier via constructive interference of the data signal and the unmodulated carrier, as we previously demonstrated in [15], achieving  $>20$  dB ER without increasing chirp; 2) employing a stronger equalizer with a longer memory length that compensates for the higher chirp associated with increased ER;

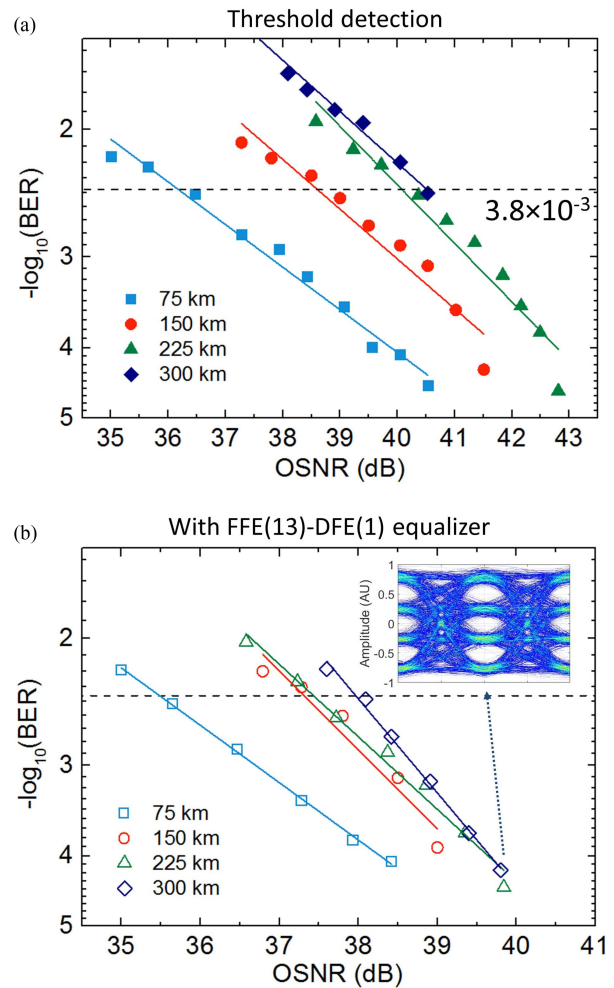


Fig. 8. Measured BER after transmission over different lengths of fiber using (a) threshold detection and (b) FFE(13)-DFE(1) equalizer. Markers in both figures: Square: 75 km; Circle: 150 km; Triangle: 225 km; Diamond: 300 km.

3) exploiting low chirp semiconductor lasers such as quantum-dot semiconductor lasers [24]. At the receiver side, performance improvement could be obtained by using a stronger equalizer such as the maximum-likelihood sequence equalizer (MLSE) at the receiver side to compensate for the PMD and residual CD [25]. The above-mentioned technologies for further performance enhancement is outside of the scope of this paper.

The moderate data rate was primarily constrained by the limited bandwidth of the FP-LDs used in the experiment. However, this does not preclude our conclusion that the concept of this new transmitter design can be extended using high-speed DMLs for high data transmission.

The proposed transmitter can be fully integrated and potentially made at low-cost and to have low power consumption. Compared to a conventional IQ modulator that contains two push-pull operated Mach-Zehnder modulator in a nested structure, the proposed transmitter only requires the driving of the two slave lasers, which significantly simplifies the photonic and electrical design as well as the transmitter packaging. The proposed simple transmitter will have a small chip size when produced in a photonic integrated circuit, which would result in more

chips per wafer which would further reduce cost under mass production. Additionally, with a driving voltage of  $1.8 V_{pp}$ , the proposed transmitter requires much less power than the conventional  $\text{LiNbO}_3$  IQ modulator.

The proposed transmitter inherently has higher output power than other transmitter schemes because it directly combines laser outputs without introducing extra insertion loss. For example, in our experiment, the proposed transmitter outputs 7 dBm power with 6 dBm master laser power, which is 6–8 dB higher than using a  $\text{LiNbO}_3$  IQ modulator. Besides, the OIL simultaneously enhances the modulation bandwidth and reduces the relative intensity noise (RIN), achieving high-performance transmitters using low-cost lasers [14]. The OIL condition including the injection power, temperature, and master-slave frequency deviation can be controlled and stabilized by a simple feedback control [26].

To compensate for the residual chirp induced amplitude-phase modulation, we measured the amplitude-phase response of OIL-DMLs and proposed a data set based method to compensate for the nonlinear field response for the first time. This approach can be applied to other semiconductor modulators such as InP IQ modulator [27] to compensate for residual amplitude-phase modulation, as we have demonstrated in [28].

## VI. CONCLUSION

We have proposed and demonstrated an OIL-DML based optical transmitter that operates in the first quadrant of the complex signal plane. The proposed transmitter can fully compensate for the CD in a direct detection system. Our proof-of-concept experiment achieved a 300-km transmission distance for a directly modulated 20-Gbit/s PAM4 signal. We believe the data rate can be improved to beyond 100-Gb/s using higher modulation bandwidth lasers, which are now available [8] and the transmission distance could be further increased through improved transmitter engineering. The proposed transmitter has all the benefits of direct laser modulation including high optical signal-to-noise ratio (OSNR), reduced power consumption, a small footprint, and ease of integration.

Although the experiment in this paper focuses on DD transmission, the proposed transmitter is naturally suitable for coherent systems. This would provide short and medium reach optical communications with a flexible transmitter that can be used reliably for both DD and coherent systems.

## ACKNOWLEDGMENT

The data are available through the UCL research depository.

## REFERENCES

- [1] F. Karinou, N. Stojanovic, and Z. Yu, "Toward cost-efficient 100G metro networks using IM/DD, 10-GHz components, and MLSE receiver," *J. Lightw. Technol.*, vol. 33, no. 19, pp. 4109–4117, Oct. 2015.
- [2] X. Chen *et al.*, "218-Gb/s single-wavelength, single-polarization, single photodiode transmission over 125-km of standard singlemode fiber using Kramers-Kronig detection" in *Proc. Opt. Fiber Commun. Conf.*, 2017, Paper Th5B.6.
- [3] S. Le *et al.*, "8 × 256 Gbps virtual-carrier assisted WDM direct-detection transmission over a single span of 200 km," in *Proc. Eur. Conf. Opt. Commun.*, 2017, Paper Th.PDP.B.1.
- [4] Z. Li *et al.*, "SSBI mitigation and the Kramers-Kronig scheme in single-sideband direct-detection transmission with receiver-based electronic dispersion compensation," *J. Lightw. Technol.*, vol. 35, no. 10, pp. 1887–1893, May 2017.
- [5] M. Birk *et al.*, "First 400GBASE-LR8 interoperability using CFP8 modules," in *Proc. Opt. Fiber Commun. Conf.*, 2017, Paper Th5B.7.
- [6] N. Eiselt *et al.*, "First real-time 400G PAM-4 demonstration for inter-data center transmission over 100 km of SSMF at 1550 nm," in *Proc. Opt. Fiber Commun. Conf.*, 2016, Paper W1K.5.
- [7] Roi Rath *et al.*, "Tomlinson–Harashima precoding for dispersion uncompensated PAM-4 transmission with direct-detection," *J. Lightw. Technol.*, vol. 35, no. 18, pp. 3909–3917, Sep. 2017.
- [8] Y. Matsui *et al.*, "55-GHz bandwidth short-cavity distributed reflector laser and its application to 112-Gb/s PAM-4," in *Proc. Opt. Fiber Commun. Conf.*, 2016, Paper Th5B.4.
- [9] S. Zhou *et al.*, "Transmission of 2 × 56 Gb/s PAM-4 signal over 100 km SSMF using 18 GHz DMLs," *Opt. Lett.*, vol. 41, pp. 1805–1808, 2016.
- [10] D. Mahgerefteh, Y. Matsui, X. Zheng, and K. McCallion, "Chirp managed laser and applications," *IEEE J. Sel. Topics Quantum Electron.*, vol. 16, no. 5, pp. 1126–1139, Sep./Oct. 2010.
- [11] E. Lau, X. Zhao, H. Sung, D. Parekh, C. Chang-Hasnain, and M. Wu, "Strong optical injection-locked semiconductor lasers demonstrating >100-GHz resonance frequencies and 80-GHz intrinsic bandwidths," *Opt. Express*, vol. 16, pp. 6609–6618, 2008.
- [12] Z. Liu *et al.*, "300-km transmission of dispersion pre-compensated PAM4 using direct modulation and direct detection," in *Proc. Opt. Fiber Commun. Conf.*, 2017, Paper Th3D.6.
- [13] T. B. Simpson, J. M. Liu, and A. Gavrielides, "Bandwidth enhancement and broadband noise reduction in injection-locked semiconductor lasers," *IEEE Photon. Technol. Lett.*, vol. 7, no. 7, pp. 709–711, Jul. 1995.
- [14] E. K. Lau, L. J. Wong, and M. C. Wu, "Enhanced modulation characteristics of optical injection-locked lasers: A tutorial," *IEEE J. Sel. Topics Quantum Electron.*, vol. 15, no. 3, pp. 618–633, May/Jun. 2009.
- [15] Z. Liu *et al.*, "Modulator-free quadrature amplitude modulation signal synthesis," *Nature Commun.*, vol. 5, 2014, Art. no. 5911.
- [16] G. Yabre, "Effect of relatively strong light injection on the chirp-to-power ratio and the 3 dB bandwidth of directly modulated semiconductor lasers," *J. Lightw. Technol.*, vol. 14, no. 10, pp. 2367–2373, Oct. 1996.
- [17] R. Slavik, J. Kakande, R. Phelan, J. O'Carroll, B. Kelly, and D. J. Richardson, "QAM synthesis by direct modulation of semiconductor lasers under injection locking," in *Proc. Opt. Fiber Commun. Conf.*, 2013, Paper JTh2A.32.
- [18] R. Lang, "Injection locking properties of a semiconductor laser," *IEEE J. Quantum Electron.*, vol. 18, no. 6, pp. 976–983, Jun. 1982.
- [19] B. W. Hakki, "Evaluation of transmission characteristics of chirped DFB lasers in dispersive optical fiber," *J. Lightw. Technol.*, vol. 10, no. 7, pp. 964–970, Jul. 1992.
- [20] F. Buchali *et al.*, "Implementation of 64QAM at 42.66 GBaud using 1.5 samples per symbol DAC and demonstration of up to 300 km fiber transmission," in *Proc. Opt. Fiber Commun. Conf.*, 2014, Paper M2A.1.
- [21] S. J. Savory, "Digital coherent optical receivers: Algorithms and subsystems," *IEEE J. Sel. Topics Quantum Electron.*, vol. 16, no. 5, pp. 1164–1179, Sep./Oct. 2010.
- [22] Z. Liu, B. Kelly, J. Ocarroll, R. Phelan, D. J. Richardson, and R. Slavik, "Discrete multitone format for repeater-less direct-modulation direct-detection over 150 km," *J. Lightw. Technol.*, vol. 34, no. 13, pp. 3223–3229, Jul. 2016.
- [23] S. Kobayashi and T. Kimura, "Optical phase modulation in an injection locked AlGaAs semiconductor laser," *IEEE Trans. Microw. Theory Techn.*, vol. 30, no. 10, pp. 1650–1657, Oct. 1982.
- [24] H. Saito, K. Nishi, A. Kamei, and S. Sugou, "Low chirp observed in directly modulated quantum dot lasers," *IEEE Photon. Technol. Lett.*, vol. 12, no. 10, pp. 1298–1300, Oct. 2000.
- [25] H. Bülow, F. Buchali, and A. Klekamp, "Electronic dispersion compensation," *J. Lightw. Technol.*, vol. 26, no. 1, pp. 158–167, Jan. 2008.
- [26] B. P. P. Kuo, E. Myslivets, V. Ataie, E. G. Temprana, N. Alic, and S. Radic, "Wideband parametric frequency comb as coherent optical carrier," *J. Lightw. Technol.*, vol. 31, no. 21, pp. 3414–3419, Nov. 2013.
- [27] R. A. Griffin, S. K. Jones, N. Whitbread, S. C. Heck, and L. N. Langley, "InP Mach-Zehnder modulator platform for 10/40/100/200-Gb/s operation," *IEEE J. Sel. Topics Quantum Electron.*, vol. 19, no. 6, Nov./Dec. 2013, Art. no. 3401209.
- [28] Z. Liu, S. Farwell, M. Wale, D. J. Richardson, and R. Slavik, "InP-based optical comb-locked tunable transmitter," in *Proc. Opt. Fiber Commun. Conf.*, 2016, Paper Tu2K.2.

**Zhixin Liu** (M'12–SM'17) received the B.Eng. degree in information engineering and the B.B.A. degree in business administration from Tianjin University, Tianjin, China, in 2006, the M.S. degree in electrical engineering from Shanghai Jiao Tong University, Shanghai, China, in 2009, and the Ph.D. degree in information engineering from the Chinese University of Hong Kong, Hong Kong, in 2012.

He joined the Optoelectronics Research Centre, University of Southampton, Southampton, U.K., in 2013. In 2016, he joined the Department of Electronics and Electrical Engineering, University College London. His current research interests include high-speed direct modulation and coherent optical signal processing with focus on phase locking, advance modulation formats, advanced multiplexing/demultiplexing schemes, and their system applications.

Dr. Liu is a senior member of OSA.

**Graham Hesketh**, biography not available at the time of publication.

**Brian Kelly** (M'15) received the B.Sc.(Hons.) degree in applied physics from Dublin City University, Dublin, Ireland, in 1990, and the Ph.D. degree in physics from Trinity College Dublin, Dublin, in 1996. His doctoral research involved the design and implementation of semiconductor optical switches in adaptive systems.

From 1996 to 2001, he was with the Optoelectronics Technology Development section, Mitsubishi Chemical, Ibaraki, Japan, where he worked on the development of high-power pump laser diodes. Since 2001, he has been with Eblana Photonics, Dublin, and is the Director of Product Development and Manufacturing. His research interests include development of robust, low-cost production methods for optoelectronic components and research into implementation of tunable single-wavelength lasers, photonic integrated lasers and high-speed transmitters for sensing, measurement, and communications.

**John O'Carroll** (M'18) received the B.Eng. and M.Eng. degrees in electronic engineering from the University of Limerick, Limerick, Ireland, in 2000 and 2003, respectively, and the Ph.D. degree from Dublin City University, Dublin, Ireland, in 2013. In 2004, he joined Eblana Photonics, Dublin, where he works as an Engineer with responsibility for laser characterisation and device applications. His current research interests include the development of high-speed directly modulated lasers for optical access networks and narrow linewidth lasers for use with advanced modulation formats.

**Richard Phelan** was born in Kilkenny, Ireland, in 1976. He received the B.Sc.(Hons.) degree in physics with lasers and photonics from the University of Hull, Hull, U.K., in 2000, and the Ph.D. degree in widely tunable semiconductor lasers and their applications from the Semiconductor Photonics Group, from Trinity College Dublin, Dublin, Ireland, in 2004. He is currently the Director of Research & Development with Eblana Photonics, Dublin, and has more than 15 years of experience in the design and fabrication of single mode laser diodes. His research interests include the design of single-mode lasers from the visible to mid-infrared, photonic integrated circuits, and high-speed direct modulation of lasers diodes for access and enterprise applications.

**David J. Richardson** (F'15) received the B.Sc. and Ph.D. degrees in fundamental physics from Sussex University, Brighton, U.K., in 1985 and 1989, respectively.

He joined the Optoelectronics Research Centre (ORC), Southampton University, in 1989, and was awarded a Royal Society University Fellowship in 1991 in recognition of his pioneering work on short pulsed fiber lasers. He is currently a Deputy Director with the ORC with responsibility for the ORC's fiber-related activities. His current research interests include amongst others: optical fiber communications, microstructured optical fibers, and pulsed high-power fibre lasers. He is a prominent figure in the international photonics community and has published more than 900 conference and journal papers and produced more than 20 patents.

Dr. Richardson is a Fellow of the Optical Society of America and the Institute of Engineering and Technology and was made a Fellow of the Royal Academy of Engineering in 2009.

**Radan Slavík** (M'07–SM'07) received the M.A.Sc. and Ph.D. degrees in optics and optoelectronics from the Faculty of Mathematics and Physics, Charles University, Prague, Czech Republic, in 1996 and 2000, respectively, and the D.Sc. degree from Academy of Sciences of the Czech Republic, Staré Město, Czech Republic, in 2009.

In 1995–2000 and 2004–2009, he was with the Institute of Photonics and Electronics, Czech Academy of Sciences in Prague. In 2000–2003, he was with the Centre d'optique, photonique et laser at Université Laval, Québec, Canada, as a Postdoctoral Research Fellow. Since 2009, he has been with Optoelectronics Research Centre, University of Southampton, Southampton, U.K. His research interests focus in optical and optics-assisted signal processing.

Dr. Slavík is a Fellow of OSA. In 2006, he was the recipient of the Otto Wichterle Award, and in 2007, the Visegrad Group Academies Young Researcher Award.